Assessing the expression of large-scale climatic fluctuations in the hydrological variability of daily Seine river flow (France) between 1950 and 2008 using Hilbert–Huang Transform

Nicolas Massei, Matthieu Fournier

Assessing the expression of large-scale climatic fluctuations in the hydrological variability of daily Seine river flow (France) between 1950 and 2008 using Hilbert–Huang Transform

Nicolas Massei *, Matthieu Fournier

Continental and Coastal Morphodynamics Laboratory, UMR CNRS 6143, University of Rouen, 76821 Mont-Saint-Aignan cedex, France

Daily Seine river flow variability from 1950 to 2008 was analyzed and compared to the winter-months North-Atlantic Oscillation (NAO) using Hilbert–Huang Transform (HHT). For the last 10 years, HHT has proven its efficiency for the analysis of transient oscillatory signals. HHT provides an interesting alterna-tive to other techniques for time-frequency or time scale analysis of non-stationary signals. In this study we aimed at delineating the different components characterizing daily flow of the Seine river, on the short-term, intra-seasonal, annual and interannual time scales and eventually interpret them in the con-text of regional North-Atlantic climate regime fluctuations. HHT results highlighted the existence of similar scales of variability beard by internal components of each NAO or river flow signal at interannual scales. Hypotheses on a possible link between the Madden–Julian Oscillation pattern and intra-seasonal variability of river flow could be also proposed, which would highlight linkages between river flow var-iability and global climate oscillations. Finally, all oscillating components were found to increase in amplitude in both climatic and hydrological signals in the end of the 1950–2008 period of study, with a first step in the late 1960s–early 1970s and a second step in the early 1990s, which demonstrated the capabilities of HHT to handle non-stationarity of natural processes and to help interpreting hydrolog-ical variability in a context of climate changes.

1. Introduction

In a context of climate and environmental changes, studying alterations of hydrological characteristics on the long-term scale has become one major issue. Increasing knowledge is needed on large-scale variations of hydrological variables and water cycle parameters in order to assess their potential impact on water resources availability and hydrologic hazards.

For the last 10 years, numerous studies investigated streamflow variability in many different regions in the world, using various approaches. In the conterminous United States, McCabe and Wolock (2002) investigated the temporal trends of streamflow variability based on a compilation of 400 daily discharge records (i.e. 395 time series) for watersheds relatively free of anthropogenic effects; they reported a step increase in streamflow around the early 1970s. Collins (2009) reached a similar conclusion of a clear change around ~1970 in his study of streamflow based on watersheds of the northeastern US. Labat et al. (2004) used wavelet analysis for investigating the variability of global runoff including potential links with climatic oscillations. In the same way, Massei et al. (2011) investigated the variability of streamflow in the Mississippi river and its main tributaries and showed that it was characterized by some significant scales of variability that could be more or less directly inherited from climate oscillations observed through selected climate indices. In the european area, Massei et al. (2007) investigated the potential relationships between the North-Atlantic Oscillation (NAO) at a daily time-step and daily precipitation in northwestern France over the past decades, suggesting some common variability scales and more importantly common characteristic time periods of either high or low variability. Later on, Massei et al. (2010) also highlighted the significant expression of similar variability scales between winter-months NAO and daily Seine river discharge, emphasizing on (and quantifying) the close relation of flow interannual variability and climate fluctuations.

In a number of those works, spectral techniques, such as Fourier spectral analyses and more recently during the past 10 years continuous and multiresolution wavelet analyses, have proven their efficiency for investigating variability scales and scaling behavior of hydrometeorological time series (Anctil and Coulibaly, 2004; Labat, 2005; Massei et al., 2007): wavelet-based techniques – either continuous or discrete – in particular, offered the possibility to better characterize the complex modalities of variation inherent to non-stationary processes. More recently, Huang et al. (1998)

* Corresponding author. Tel.: +33 232 769 443.
E-mail address: nicolas.massei@univ-rouen.fr (N. Massei).

developed the so-called Hilbert–Huang Transform (HHT), an approach associating a newly developed multiresolution decomposition method named empirical mode decomposition (EMD), and the Hilbert transform for detecting changes in the variability scales across the signal analyzed. In Earth sciences, HHT has been already applied in the field of atmospheric sciences, oceanography and hydrological sciences (Peel and McMahon, 2006; McMahon et al., 2007; Breaker et al., 2008; Sole et al., 2009; Franceschini and Tsai, 2010; Lee and Ouarda, 2010, 2011). One of the main flaw of EMD consisted of mode mixing between separated components, i.e. the distribution of the same scale of variability across several components. Wu and Huang (2009) then proposed an improvement of EMD called Ensemble EMD (EEMD) which proved much better capabilities for extracting a limited number of physically meaningful components of a signal. A synthesis on the principle, recent methodological development and application of the Hilbert–Huang Transform is provided in Huang and Wu (2008).

Huang et al. (2009) already investigated the scaling behavior of Seine river flow and compared it to a small river in northern France, the Wimereux river, using EMD and Hilbert Spectral Analysis (HSA). These authors proposed a methodology for HSA based on the generalization of the Hilbert marginal spectrum for arbitrary order moments and refined the analysis of the scaling behavior of the Seine and Wimereux river using an extended-self-similarity approach. They eventually concluded to a higher degree of multifractality and smaller scaling exponent for the small watershed, which they interpreted in terms of larger inertia of the bigger Seine watershed.

In this paper we focus on the characterization of the climatic determinism in Seine river flow by comparing its variability it to that of the NAO index. We investigate the aptitude of HHT for characterizing the variability, detecting singularities and changes in daily Seine river flow (France) in relation with climate fluctuations in the North Atlantic as described by the NAO index. We aim to define what internal components can be detected and extracted by the non-parametric, auto-adaptive and orthogonal EEMD in daily Seine river flow and annual NAO index, and assess the potential links between changes in Seine flow variability and recent changes in climate fluctuations thanks to EEMD and to the determination of instantaneous frequency trajectories by Hilbert transform.

2. General principles of the Ensemble Empirical Mode Decomposition and the Hilbert–Huang Transform

The Hilbert–Huang Transform is a non-stationary data processing method developed by Huang et al. (1998) which combines the so-called Empirical Mode Decomposition (EMD) multiresolution analysis (and more specifically its improvement, i.e. EEMD/Ensemble Empirical Mode Decomposition) and the Hilbert transform in order to achieve a time-frequency analysis of a given signal. It basically stands in two steps: (1) the decomposition of the time series considered in IMFs (Intrinsic Mode Functions) by an empirical multiresolution analysis technique called EMD (Empirical Mode Decomposition), (2) the determination of the time-varying instantaneous frequency associated to each IMF by calculation of its Hilbert transform in order to achieve a time-frequency visualization of the signal amplitude through time. In this study we used the EMD R package by Kim and Oh (2009), the HHT Matlab program provided by Wu and Huang (2009), and we eventually implemented the EEMD procedure in R.

2.1. The Empirical Mode Decomposition (EMD) and Ensemble EMD (EEMD)

The basic principle of EMD consists in extracting the orthogonal intrinsic oscillatory modes (the IMFs) constituting the signal $x(t)$ to be analyzed. Basically, an IMF is a function that satisfies two conditions: (a) the number of extrema and the number of zero crossings in the signal must either equal or differ at most by one, (b) at any point, the mean value of the envelope defined by the local maxima and the envelope defined by the local minima is zero. Extraction of the IMFs is performed by an iterative procedure defined as the sifting process. In practice, the sifting process consists of the following steps repeated n times from $k = 1$ to n, n being the total number of IMFs:

1. Identify the local extrema in the original signal $x(t)$ to get an upper and a lower envelope. These envelopes are actually obtained by performing a cubic spline interpolation over the successive maxima (upper envelope) or minima (lower envelope) across the signal.
2. Compute the local mean value of the maxima and minima envelopes, which gives a mean series $m_1(t)$ and subtract it from the signal $x(t)$, which gives a function $h_1(t)$. If $h_1(t)$ satisfies the requirement (a) and (b) above, than $h_1(t)$ is the first IMF $imf_1(t)$ of the signal $x(t)$. If $h_1(t)$ does not meet requirements (a) and (b), the steps (1) and (2) are repeated with $h_1(t)$ instead of $x(t)$ until one function $h_i(t)$ is eventually identified as the first IMF $imf_1(t)=h_i(t)$. Steps 1- and 2-may be repeated i times within each step k in order to identify the kth IMF.
3. The first residual $r1(t)$ resulting from the substraction of $imf_1(t)$ from $x(t)$ at $k = 1$ is then passed through steps 1- and 2-iteratively until the last function $h_i^k(t)$ computed cannot meet the requirements (a) and (b): at this last step $k = n$, all the original signal has been decomposed into n IMFs and a residue $r(t)$ (Eq. (1)).

$$x(t) = \sum_{k=1}^{n} imf_k(t) + r(t) \tag{1}$$

The residue $r(t)$ represents the trend existing in the signal $x(t)$ and is not parametrically defined unlike with polynomial fitting or LOESS smoothing as utilized in Massei et al. (2010) on the same data, for instance.

In order to avoid a distribution of the same scales amongst different IMFs as a result of intermittency in the original signal, that may alter interpretation of the physical meaning of IMFs, Wu and Huang (2009), inspired by works from Flandrin et al. (2004) and Gledhill (2003), improved the EMD algorithm and developed the so-called Ensemble Empirical Mode Decomposition (EEMD) which consists of a noise-assisted data analysis method . Indeed, Flandrin et al. (2004) and Wu and Huang (2004) showed that the EMD method is effectively an adaptive dyadic filter bank when applied to white noise. In brief, the principle of EEMD relies of adding noise in the original data, which provides a uniformly distributed reference scale in the initial series and then cancel the problem of intermittency in the decomposition via the EMD filter bank. Added white noise is eventually removed by averaging on (taking the ensemble mean of) the decomposed IMFs over a large number of decompositions, each involving the original signal altered with a different white noise each time (Wu and Huang, 2004, 2009). Up to now, EEMD has been only used in a few amount climate/hydrological studies such as Lee and Ouarda (2010, 2011).

2.2. Determination of instantaneous frequencies by Hilbert transform

One interest of the Hilbert–Huang Transform lies in the fact that applying the Hilbert transform to the identified IMFs allows a time-frequency representation of the energy associated to each IMF. It is then possible to achieve an orthogonal decomposition of the signal analyzed by EMD in a similar way as discrete wavelet

multiresolution analysis and to obtain a time-frequency diagram, similarly as the time-scale diagram obtained by continuous wavelet transform, by calculation of each IMF's Hilbert transform. A short comparison between these different approaches will be given later in the discussion section.

The Hilbert transform $y(t)$ of a real-valued function $x(t)$ is defined as:

$$y(t) = \frac{1}{\pi} P \int_{-\infty}^{+\infty} \frac{x(\tau)}{t-\tau} d\tau \tag{2}$$

where P is the principal Cauchy value. The complex-valued analytic signal $s(t)$ associated to $x(t)$ is:

$$s(t) = x(t) + i \cdot y(t) \tag{3}$$

or:

$$s(t) = a(t) \cdot e^{i\varphi(t)} \tag{4}$$

with

$$a(t) = \sqrt{x(t)^2 + y(t)^2} \tag{5}$$

and

$$\varphi(t) = \arctan\left(\frac{x(t)}{y(t)}\right) \tag{6}$$

The so-called instantaneous frequency is defined as:

$$\omega(t) = \frac{1}{2\pi} \frac{d\varphi(t)}{dt} \tag{7}$$

Each IMF is then associated to an instantaneous frequency function $\omega(t)$. One eventually obtain a time–frequency–energy diagram for each IMF that reads in a similar way as a continuous wavelet spectrum.

3. Hydroclimatic data

3.1. Daily flow data of the Seine river watershed

The Seine river is 777 km in length and drains an area of about 78,650 km^2. Its watershed is characterized by intensive agricultural activities and by the presence the city of Paris. In its entirety, the Seine river watershed gathers a little less than 30% of the French total population (i.e. nearly 20,000,000 inhabitants). The Seine river discharges into the English Channel near the city of Le Havre through a megatidal estuary. As a result, flow assessment is made virtually impossible at the very downstream part of the river. On the other hand, data are available at Poses, a small town upstream of the city of Rouen, more precisely at the level of the Poses lock (dam), which is located 160 km upstream from the estuarine mouth and corresponds to the tidal limit of the Seine estuary. Since 1941 the "Service de la navigation en Seine" (Seine navigation office) provides daily data of River flow measurements achieved 1 km upstream of the lock (Fig. 1, top panel). Before 1995 estimation of the river flow was achieved once a day by measuring the slope between Poses and the other upstream locks. This technique was based on two rating curves for low and high river flow conditions. The two curves were not totally recovering for river flow between 900 and 1000 m^3 s^{-1}. As a consequence this range of river flow may have been slightly underestimated before 1955. Since 1995 an ultrasound probe (one burst every 15 mn) provides accurate river flow measurements. Overall between 1950 and 2008, daily Seine river flow is 445 m^3 s^{-1} on average and its standard deviation is 329.6 m^3 s^{-1}. Over the 1950–2008 period of study, flow ranged from 40 m^3 s^{-1} up to nearly 2300 m^3 s^{-1}.

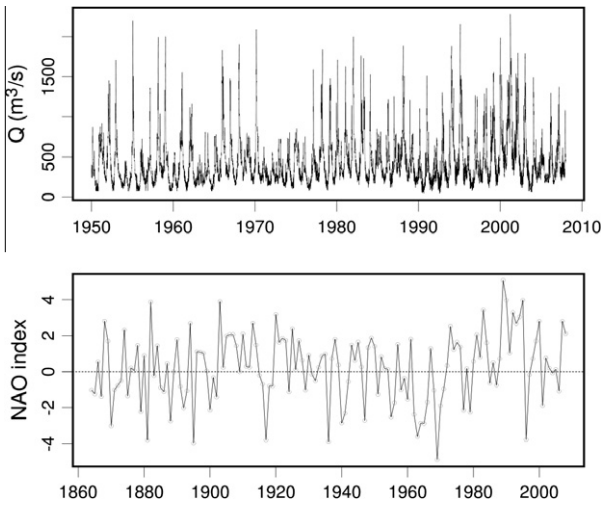

Fig. 1. Daily Seine river flow time series (upper panel) and annual winter-months NAO index (lower panel).

3.2. The North-Atlantic Oscillation

In Europe, the North-Atlantic Oscillation (NAO) reflects the main fluctuations of climatic conditions (Hurrell and Van Loon, 1997). As described by Hurrell et al. (2003), "The NAO refers to a redistribution of atmospheric mass between the Arctic and the subtropical Atlantic, and swings from one phase to another produce large changes in the mean wind speed and direction over the Atlantic, the heat and moisture transport between the Atlantic and the neighboring continents, and the intensity and number of storms, their paths, and their weather. Agricultural harvests, water management, energy supply and demand, and yields from fisheries, among many other things, are directly affected by the NAO". The NAO reflects the main fluctuation of climatic conditions in Europe and also affects the eastern/northeastern coast of North America: during positive NAO, these regions undergo wetter weather conditions and conversely for negative NAO.

The relationships between NAO and both global and local weather patterns such as precipitation and storm track activity (Rogers, 1997; Ulbrich et al., 1999; Mares et al., 2002; Keim et al., 2004), but also ecosystems dynamics (Parsons and Lear, 2001; Greene et al., 2003; Lomas and Bates, 2004), contaminant transport in the atmosphere (Macdonald et al., 2005) are wide and complex. This highlights the major interest of investigating the temporal variations of this climatic indicator, accurately detect their modalities and confront them to the leading modes of hydrological characteristics variations. Bradbury et al. (2002) studied the relationships between monthly NAO and streamflow in New England (East coast of the USA) and suggested that such relationships would be better expressed in the lower frequency part of their respective spectra. Kingston et al. (2007) underlined a probable positive relationship between the NAO and New England streamflow, but at the same time strongly suggested that further research would be needed to get deeper insights into the complex NAO–streamflow link, which appears definitely not straightforward according to these authors. In this sense, some of our previous works highlighted the existence of some potential links between NAO fluctuations and hyhydrological signals in northwestern France: interannual patterns similar to those that characterize NAO were detected in precipitation (Massei et al., 2007; Fritier et al., 2010), streamflow of the Seine river (Massei et al., 2010) and also in the variability of the Chalk aquifer groundwater ressources (Slimani et al., 2009).

In the present study the annual winter-months NAO index available at http://www.cgd.ucar.edu/cas/jhurrell/indices.html was used (Fig. 1, bottom panel), which is computed from the station-based sea

level pressure (SLP) difference for winter months (December through March:) between Lisbon, Portugal and Stykkisholmur/Reykjavik, Iceland since 1864. SLP anomalies at each station is normalized by dividing each seasonal mean pressure by the long-term (1864–1983) mean standard deviation.

4. Determination of the leading scales of variability characterizing daily Seine river flow variations from 1950 to 2008

4.1. Intrinsic components of daily Seine river flow and energy distribution

EEMD of daily Seine river flow lead to the detection and extraction of 13 IMFs (or components) and a residue (Fig. 2). Some of these components clearly highlight strong intermittency: for instance, components C3–C6 are characterized by very localized peaks, and component C6 is also affected by a relatively low variability roughly between 1970 and 1980. One can notice that, contrary to what was obtained by Huang et al. (2009) using EMD on the Seine river also, the EEMD algorithm seems to actually act rather well as a dyadic filter bank (Fig. 3): the evolution of mean frequency with IMFs obeys a power law of the form

$$\omega(n) = \gamma^{-n} \tag{8}$$

with $\gamma = 2.06$.

The distribution of energy given by the various components of Seine river daily flow obtained by HHT displayed a similar scaling behavior when compared to a Fourier transform of the same signal (Fig. 4). Various power law ranges of scale invariance show up both on the Fourier spectrum and the HHT: (1) a short-term, lower than 7-day range, (2) from 7 days to intra-seasonal (∼31 days), (3) intra-seasonal scales to annual/sub-annual scales, (4) from annual/sub-annual to pluridecadal scales. These different scale ranges are separated by dashed lines in Fig. 4. One can notice the very good accordance between the distribution of energy obtained from HHT and the Fourier spectrum.

The first two scale ranges would correspond well to the response of the Seine river watershed to synoptic events, obviously modulated by the physiographical characteristics of the watershed. Concentration times on the Seine watershed range between 2 and 3 days for the very downstream part and around 13 days for the most upstream sub-watersheds. A simple cross-correlation between mean daily precipitation on the watershed and flow gives a

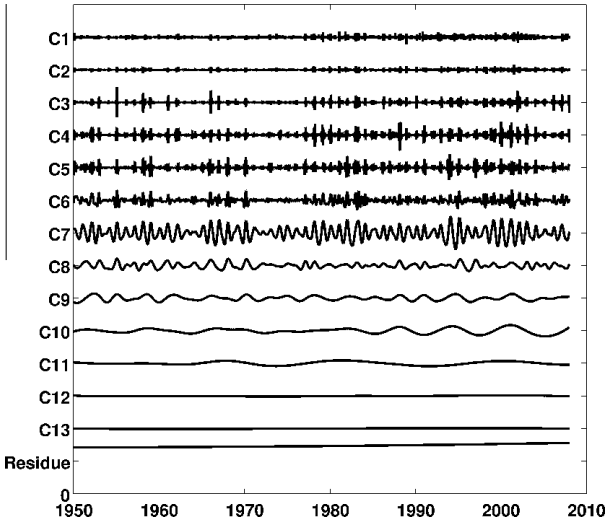

Fig. 2. EEMD of daily Seine river flow from 1950 to 2008.

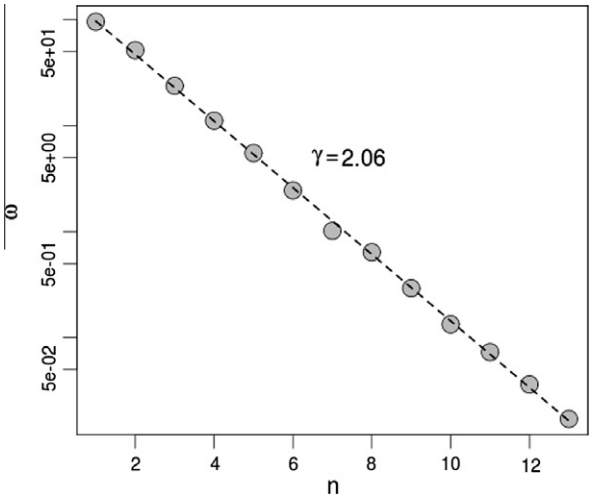

Fig. 3. Decreasing frequency with increasing order of the IMFs. The evolution of mean frequency with IMFs obeys a power law of the form $\omega(n)=\gamma - n$ with $\gamma = 2.06$, showing that the EEMD algorithm acts as a dyadic filter bank.

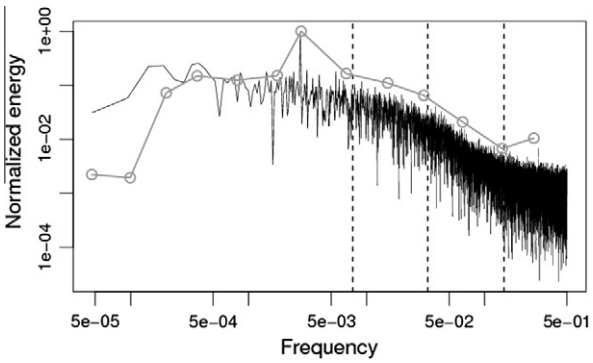

Fig. 4. Fourier energy spectrum (black solid line) and Hilbert Spectrum based on EEMD of daily Seine river flow. Dotted vertical lines indicate the detected range of scale invariance.

reasonable idea of the average flood following precipitation at a daily scale (Fig. 5): it indicates a peak time of ∼9 days and a peak duration of less than 50 days. Time scales lower than 7 days would then correspond to the most rapid increase in streamflow monitored, i.e. probably linked to the most downstream, higher concentration time parts of the Seine watershed. These most rapid events then represent flow resulting almost directly from precipitation. The longer 7–31-day scales, on the other hand, would be related to the response of longer concentration time parts of the watershed. Flow variability within this range of time scales would strongly reflect the physically-modulated response of the watershed.

Between 31 days and ∼100 days, another range of time scales shows up. The HHT spectrum clearly indicates that power in this range is gathered within components 4 and 5, i.e. around time scales of ∼33 and ∼66 days respectively. These time scales seem too long to be associated to synoptic activity; their expression in Seine river flow as a distinct range of scale invariance would rather represent intra-seasonal variations, possibly related to more global climate fluctuations as suggested in Huang et al. (2009) for the same river.

Beyond time scales superior to ∼100 days, components C6 and C7 correspond to the annual cyclicity and its semi-annual harmonic (respectively ∼359 days and ∼149 days on average), whereas at interannual scales, components C8 to C13 would indicate fluctuations linked to the oscillations of global climate as it could be

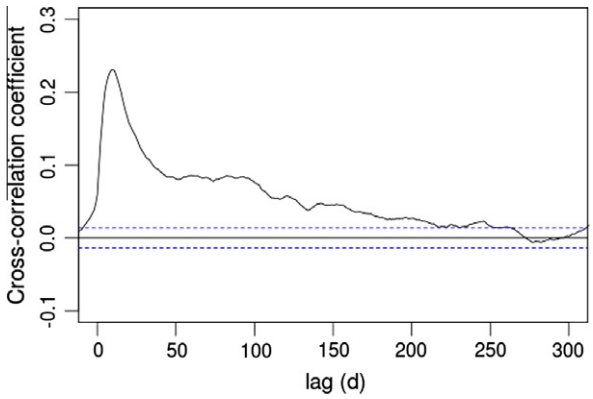

Fig. 5. Cross-correlation function between daily mean precipitation averaged over the Seine watershed and daily river discharge.

demonstrated by Massei et al. (2010). Once all IMFs have been detected, a residue indicates a slight, monotonous increase of flow.

4.2. Instantaneous frequency trajectories of the IMFs for characterizing non-stationarity of Seine river flow

The Hilbert–Huang Transform applied to each component provide information of the temporal changes in variance or amplitude at each time scale determined, which can be visualized by plotting the instantaneous frequency trajectory associated to each IMF (Fig. 6). On these plots, for reading convenience the *y*-axis actually indicates, the natural logarithm of instantaneous period (that is, $\log[1/\omega(t)]$) in years instead of instantaneous frequency, which means that ordinate 0 is 1 year on the figure; the color scale indicates the distribution of amplitude (in cubic meters per second) with time and frequency for each component. Several main conclusions can be drawn from these results:

- For the highest frequency components C1 and C2 (corresponding to scales ∼4 and ∼7 days), increasing amplitudes are visible from ∼1990 to 2008.
- The annual cycle (component C7) is well detected, concentrating amplitudes around ∼359 days on average. Higher amplitudes (of the order of 400–500 $m^3\,s^{-1}$) are identified very localized in time: for instance, around 1980, in the mid-90s and the very beginning of the 2000s.
- Interannual component C10 around 7.48 years is affected as well by an increase in amplitude from the late 80s-early 90s up to 2008. Component C10 corresponds to flow rates ranging from ∼125 $m^3\,s^{-1}$ to 200 $m^3\,s^{-1}$ between 1990 and 2008. Such an increase is non-negligible, recalling here that mean Seine river flow is 445 $m^3\,s^{-1}$ and standard deviation is 329.6 $m^3\,s^{-1}$ during this period. This also the case for the C11 component (∼13.69 years), with amplitudes around 20 $m^3\,s^{-1}$ before 1970 reaching ∼80–100 $m^3\,s^{-1}$ afterward.

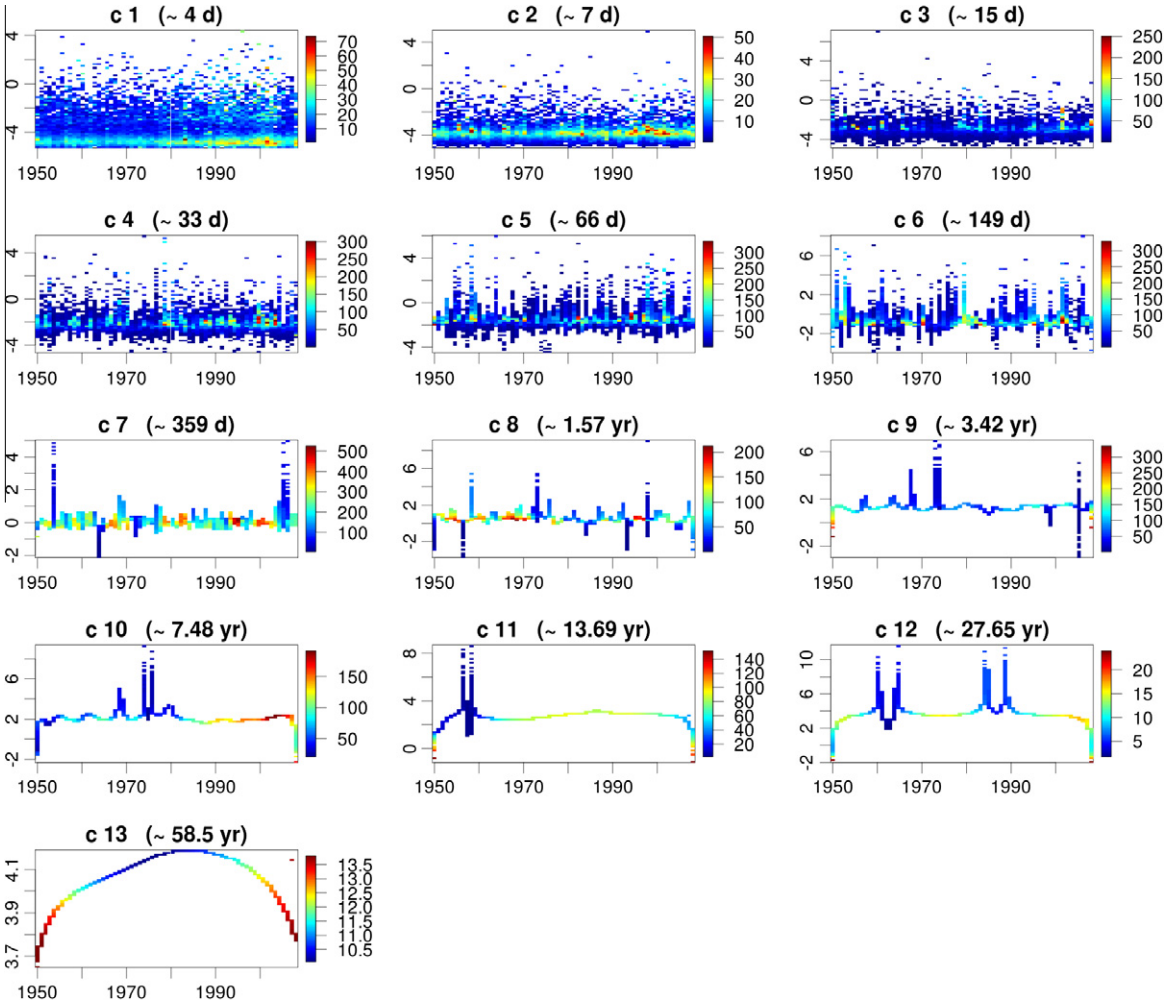

Fig. 6. Instantaneous frequency trajectories from Hilbert–Huang Transform (HHT) applied to each component (IMF) of daily Seine river flow extracted from EEMD. The color scale indicates amplitudes expressed in $m^3\,s^{-1}$.

– Singularities are detected in the form of abrupt changes in the instantaneous period, for instance around the mid-1970s for C8, C9, C10.

For all components but two (the C8 and C9 of mean period respectively equal to 1.57 and 3.42 years), the calculated amplitudes are increasing through time as indicated by a simple trend analysis using linear regression on the data (Table 1).

As a methodological parenthesis, it is informative at this stage to compare the instantaneous frequency trajectories obtained from EMD (Fig. 7) to those used here subsequently to EEMD (Fig. 6). Although, fortunately, the main characteristics are recovered, mode mixing consecutively to EMD is clearly visible in a number of cases, that can substantially alter the interpretation of any physical meaning of the IMFs: for instance, the distribution of amplitudes in component C1 is much less concentrated around the

Table 1
Mean period, amplitude and linear regression trend test for each IMF (= component) of daily Seine river flow.

	Mean period	Mean amplitude ($m^3 s^{-1}$)	Slope ($m^3 s^{-1} year^{-1}$)	F	*p*-value
C1	~4 d	25	0.26	1178.10	<2.2e-16
C1	~7 d	20	0.16	550.80	<2.2e-16
C3	~15 d	35	0.36	351.64	<2.2e-16
C4	~33 d	62	0.54	348.31	<2.2e-16
C5	~66 d	80	0.38	146.24	<2.2e-16
C6	~149 d	98	0.39	179.59	<2.2e-16
C7	~359 d	242	1.1	652.90	<2.2e-16
C8	~1.57 years	94	−0.8	1771.60	<2.2e-16
C9	~3.42 years	85	−0.6	2205.30	<2.2e-16
C10	~7.48 years	93	2.2	38266.00	<2.2e-16
C11	~13.69 years	65	0.97	9750.50	<2.2e-16
C12	~27.65 years	11	0.08	2241.70	<2.2e-16
C13	~58.5 years	11	0.008	284.92	<2.2e-16

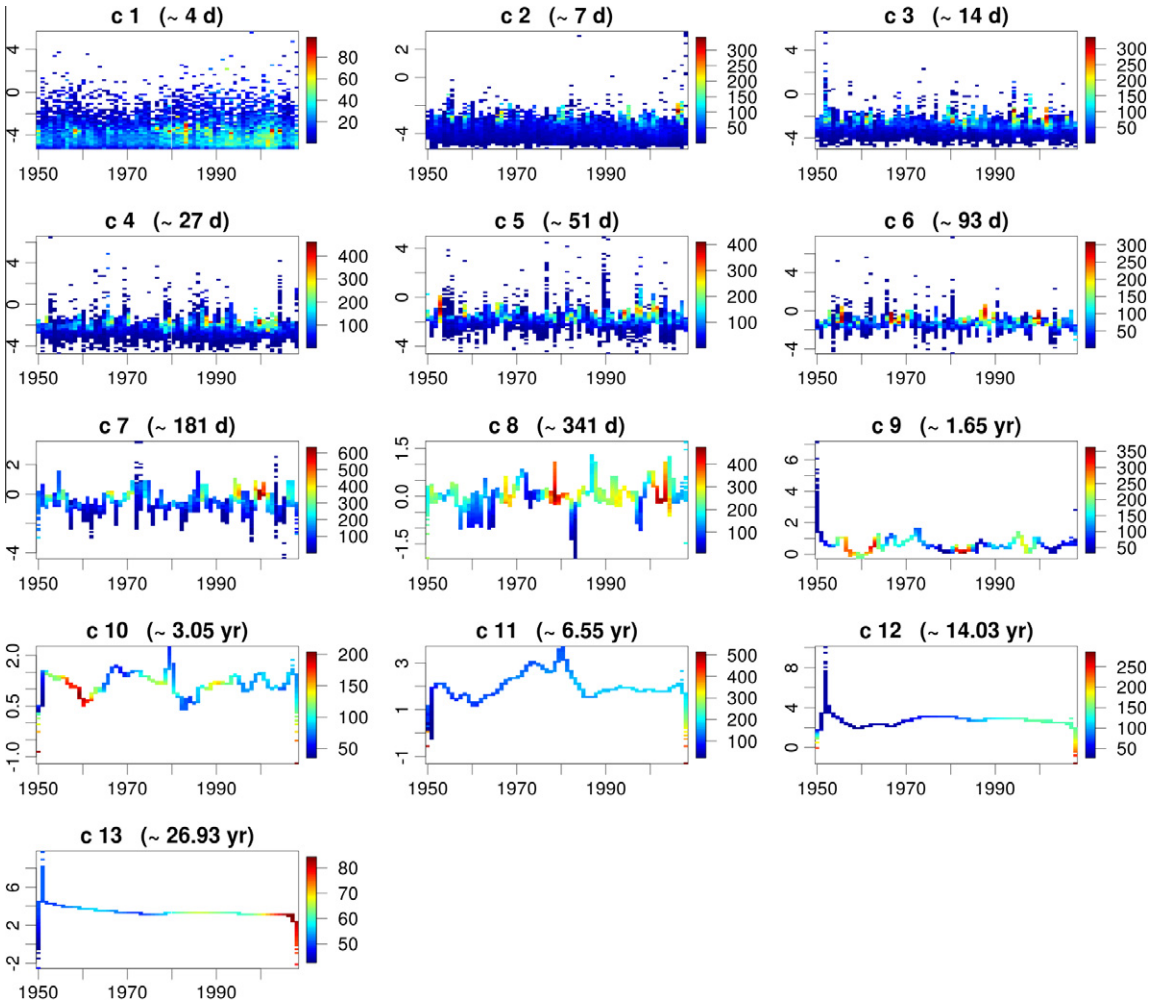

Fig. 7. Instantaneous frequency trajectories from Hilbert–Huang Transform (HHT) applied to each component (IMF) of daily Seine river flow extracted from EMD instead of EEMD. The color scale indicates amplitudes expressed in $m^3 s^{-1}$.

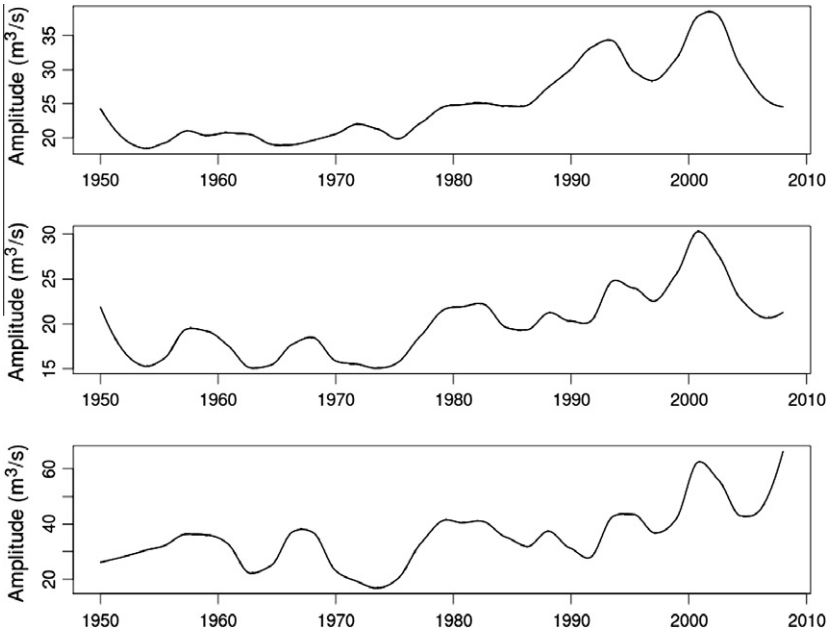

Fig. 8. Temporal distribution of amplitudes for the first three components of daily Seine river flow. Amplitudes increase significantly since the mid-1970s and seem modulated by an interannual scale of variability, leading to a pseudo-periodicity of the short-term amplitudes.

mean period of 4 days, and the annual cycle is distributed over three components (C7, C8, C9).

The increasing amplitudes in the end of the 1950–2008 period of study for the short-term components C1, C2 and C3 deserve a closer investigation. For all three components, there is a clear increase from the beginning of the 1970s. These short-term scales inferior to 15 days represent the fastest response of the watershed to precipitation as illustrated by the precipitation/river flow cross-correlation (Fig. 5). We analyzed the temporal distribution of amplitudes for components C1, C2 and C3 using local polynomial regression (LOESS algorithm) in order to investigate the variability in the short term (Fig. 8). In some previous works, Massei et al. (2011) emphasized a longer-term control on the evolution of short-term flow events of Mississippi river flow using the same approach. Here, smoothing over 20% of those noisy data actually revealed the existence of lower frequency structures controlling the variability of these components at interannual scales of about 6–8 years, which would in fact correspond rather well to an amplitude modulation by the C10 ∼7.48 year component. The intensity of short-term events in daily flow would then also be clearly controlled by interannual processes.

5. Hypotheses on a climatic control on daily flow variability of the Seine river

On interannual scales, Massei et al. (2010) already suggested a possible link between daily Seine river flow and NAO variability based on the comparison of their continuous wavelet transforms. Here we propose a characterization of NAO variability using EEMD/HHT applied to the winter-month annual NAO index time series from 1864 to 2008. The EEMD multiresolution decomposition leaded to six components and a residue (Fig. 9), on which HHT was applied in order to determine the corresponding characteristic time scale. The resulting Hilbert–Huang spectra display the instantaneous frequency trajectories associated to each IMF extracted (Fig. 10): the mean periods calculated for components C'1–C'6 are respectively 2.67, 5.88, 13.33, 30.77, 76.92 and 133.33 years (the latter corresponding to the length of the series).

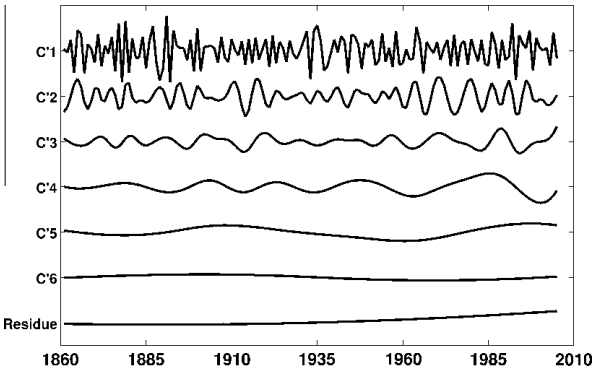

Fig. 9. EEMD of the winter-months annual NAO index time series from 1865 to 2008.

Four of these six components (C'2–C'5) are characterized by a significant increase in amplitude after approximately 1960 (Fig. 10).

Following these results, some NAO components appear to vary according to approximately the same time scale as Seine river flow. A graphical comparison illustrates those variations (Fig. 11):

1. Components C10 (∼7.48 years in Seine flow over 1950–2008) and C'2 (∼5.88 years in NAO over 1865–2008) display striking similarities (Fig. 11a). Positive NAO anomalies at this scale correspond well to flow excess, which is in accordance with the expected physical impact of NAO in the northern european region. Although Massei et al. (2010) also reached the same result using continuous wavelet transform and reconstruction, EEMD definitely proved here to perform much better. NAO and Seine flow variations do not match during the 1970s, which was also highlighted by Massei et al. (2010): this period is known worldwide as one major climate shift in the North Atlantic, closely linked to a change in the thermohaline circulation in the Atlantic (Dima and Lohmann, 2010) and that strongly impacted ecosystems at the global scale (Alexander et al., 2008; Alheit and Niquen, 2004; Daskalov, 2003; Dickson and Osterhus, 2007; Serreze et al., 2000).

2. Components C11/C'3 (~13–14 years), on the other hand, seem to vary almost out of phase (Fig. 11b). This result had also been highlighted through the comparison of NAO and precipitation in the Seine river watershed by wavelet coherence (Fritier et al., 2010). On such a time scale, it would then appear that positive NAO would not lead to wetter than usual conditions in this area as usually expected in northern european regions. As a matter of fact, the impact of NAO is not very distinctive in northern France, which is a transition zone with respect to this climate pattern.
3. Components C12/C'4 (~27–30 years) also seem to vary out of phase (Fig. 11c). This characteristics is much less clear, however, between approximately 1980 and 1990. In Seine river flow, this component has a significantly lower amplitude compared to the previous ones (C11 and C10).

The residue of EEMD applied to Seine river flow enlighted the presence of a trend in the daily flow time series. This trend delineates a progressive change from below- to above-average values of flow and its significance is not easy to interpret as is. However, comparison with the C'5 of NAO (mean period ~76.92 years) enlight a similar temporal evolution, with an increase starting in the early 1970s and a zero-crossing in the vicinity of the early 1980s (Fig. 11d). This would strongly suggest that the trend estimated in daily Seine river flow over the period 1950–2008 could be actually linked to a larger scale NAO fluctuation, hence denoting a reversible phenomenon.

In their analysis of Seine river flow on a time period (1976–2008) shorter than used in the current study (1950–2008), Huang et al. (2009) identified a range of scale invariance between 4.5 days and 60 days in the Seine river Fourier spectrum, i.e. between synoptic and intra-seasonal scales. According to the 60 days upper limit, these authors suggested a possible relation between Seine river flow and the Madden–Julian Oscillation (MJO), since the MJO wave packet propagates eastwards around the globe with a typical 30–70-day cycle as recalled by Cassou (2008). Although the MJO is rather known to have an influence on the East and West Pacific coast climate, Cassou (2008) demonstrated that the MJO would partly control the distribution of the four daily weather regimes defined over the North Atlantic–European region in winter (i.e. the so-called NAO+, NAO−, Atlantic ridge and Scandinavian blocking), and would even more particularly affect the two daily NAO+ and NAO− regimes. In the results presented here, the Fourier spectrum of daily Seine flow would display two distinct scale ranges on both sides of ~31 days, which would be confirmed by the distribution of energy given by the HHT spectrum (Fig. 4). The scale range encompassed by components C4 (33 days) and C5 (66 days) would then possibly correspond to the 30–70-day typical scale of

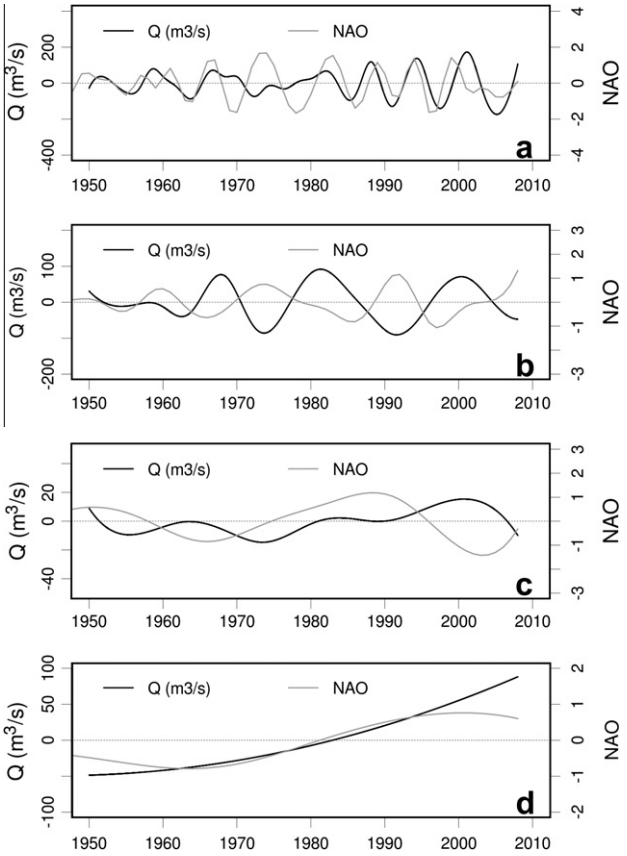

Fig. 11. Comparison between daily flow and winter-months NAO interannual components obtained from EEMD. The lower panel represents the Seine river flow EEMD residue (black line) and the ~77-years long-term component of NAO.

variability of MJO through NAO, more especially as we previously provided some evidence of a potential link between NAO and Seine flow variability. Note that using EMD instead of EEMD did not allowed identification of components at these time scales (Fig. 7).

Grouping internal components following the interpretations exposed above eventually lead to a separation of the Seine flow 1950–2008 hydrograph as displayed in Fig. 12, where one can distinguish an intra-seasonal variability possibly related to the Madden–Julian Oscillation, an annual/semi-annual component, and some interannual variability linked NAO. MJO and NAO-like fluctuations in Seine river flow would reflect the imprint, not only of North-Atlantic but also global climate oscillations in hydrological processes. It is also readily visible in Fig. 12 that the 1970s period,

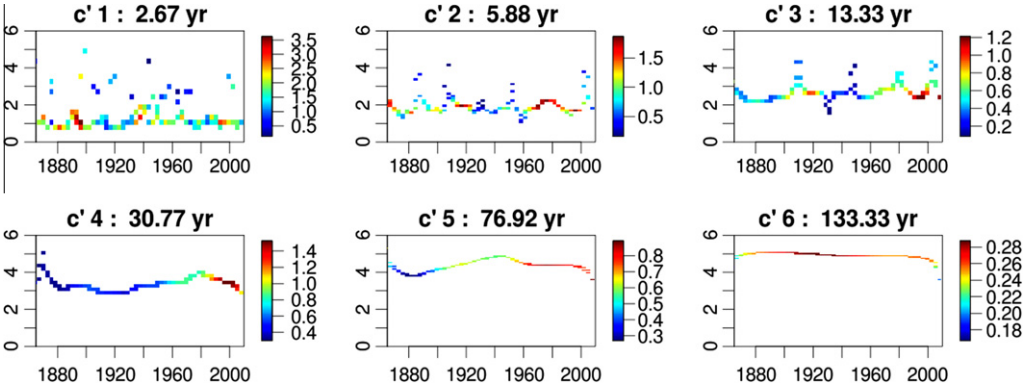

Fig. 10. Instantaneous frequency trajectories from Hilbert–Huang Transform (HHT) applied to each component (IMF) of winter-months NAO extracted from EEMD. The color scale indicates normalized unit of the NAO index.

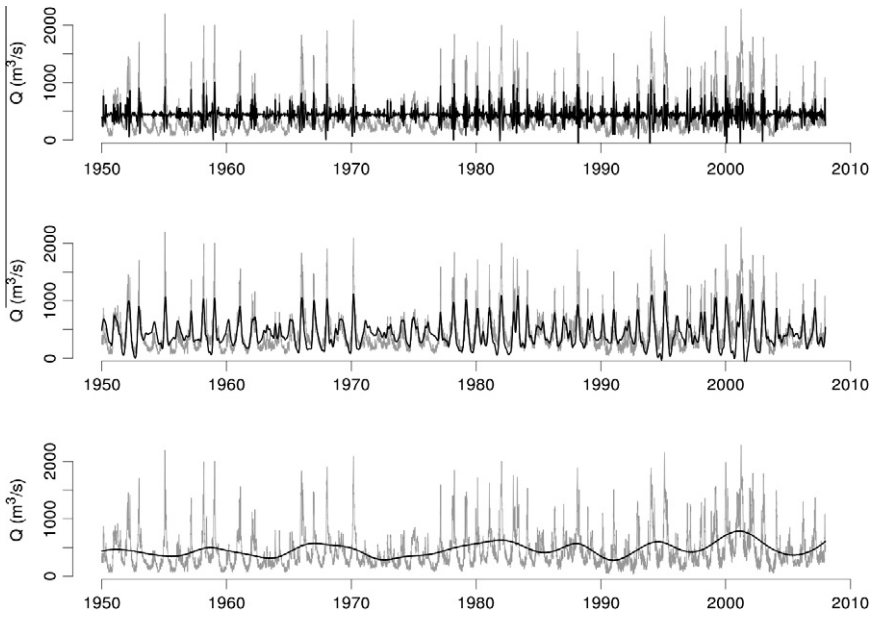

Fig. 12. Synthesis of intra-seasonal, annual/semi-annual, interannual components and trend of Seine river flow. The upper panel displays intra-seasonal components of ∼33 days and ∼66 days that might be related to the expression of the Madden–Julian Oscillation. The middle panel represents the annual and semi-annual variability. The lower panel shows the interannual the sum of components C10 (∼7.48 years), C11 (∼13.69 years), C12 (∼2765 years) and the residue of EEMD of daily Seine river flow, grouped according to their similarity with NAO components.

corresponding to one abrupt climate shift at the global scale, is a period of low amplitudes in river flow at all time scales. In addition, this 1970s period marks the transition to a higher variability in river flow studied as emphasized by increasing amplitudes of interannual components on instantaneous frequency trajectories (Fig. 6), in agreement with changes in NAO (Fig. 10).

6. Conclusion

In this study, we investigated the capability of EEMD to detect physically meaningful internal components explaining the variability of daily flow in a regional-scale watershed in the northern half of France. Indeed, previous investigations of time-scale hydrological variations of Seine flow using continuous wavelet transform provided reference for comparing the results obtained in this study.

EEMD revealed to act as a dyadic filter bank. Comparison of the Hilbert spectrum resulting from Hilbert–Huang Transform applied to each identified IMF with a Fourier energy spectrum of Seine river flow highlighted the same type of scaling behavior, with a multifractal behavior associated to different ranges of scale invariance. However, compared to the Fourier approach, HHT allowed concentrating the energy of the hydrological process analyzed on well-defined components (= IMF), each related to a specific time scale. The analysis of instantaneous frequency trajectories of each component revealed for most of them a significant increase in amplitude.

Conducting the same approach for the analysis of annual winter-months NAO variability for the period 1865–2008) leaded to the identification of components that displayed some similar characteristics as those of river flow in terms of time scale of variability and non-stationarity, with increasing amplitudes starting from the 1970s. According to these, it was possible to suggest reasonable hypotheses on the expression of region (i.e. North-Atlantic) to global climate fluctuations in hydrology of the Seine river, involving the NAO pattern in particular. This is also consistent with some previous results obtained using wavelet approaches, although EEMD/HHT proved to perform much better for detecting characteristic scales of variability, singularities and changes in variance. In addition, we also suggest that the intra-seasonal variability of Seine river flow could be linked to the Madden–Julian Oscillation, inasmuch as (1) EEMD allowed detection of flow components which varied on the same typical time scale as MJO (i.e. a scale range between ∼33 days and ∼66 days), (2) the recent literature gave evidence of a connection between MJO and NAO.

A trend in Seine flow is detected as a residue of EEMD which appears non-negligible over the period 1950–2008: according to this trend, river flow would increase by $\sim 150\,m^3\,s^{-1}$ between 1950 and 2008. However, this trend was also found to match adequately a longer-term (∼76.92 years) component of NAO variability, denoting a reversible phenomenon. However, the increasing variability determined by EEMD/HHT for both river flow and NAO since ∼1970, along with another in the early 1990s, seems, according to the changes in NAO variability since 1865, to be a recent phenomenon possibly related to recent climate change.

Acknowledgements

The authors would like to thank the Seine-Aval Regional Scientific Program for financial support.

References

Alexander, M., Capotondi, A., Miller, A., Chai, F., Brodeur, R., Deser, C., 2008. Decadal variability in the northeast Pacific in a physical-ecosystem model: role of mixed layer depth and trophic interactions. J. Geophys. Res. – Oceans 113.

Alheit, J., Niquen, M., 2004. Regime shifts in the Humboldt Current ecosystem. Progr. Oceanogr. 60, 222.

Anctil, F., Coulibaly, P., 2004. Wavelet analysis of the interannual variability in southern québec streamflow. J. Climate 17, 163–173.

Bradbury, J.A., Dingman, S.L., Keim, B.D., 2002. New England drought and relations with large scale atmospheric circulation patterns. J. Am. Water Resour. Assoc. 38 (5), 1287–1299.

Breaker, L.C., Broenkow, W.W., Watson, W.E., Jo, Y.H., 2008. Tidal and nontidal oscillations in Elkhorn Slough, CA. Estuaries Coasts 31 (2), 239–257.

Cassou, C., 2008. Intraseasonal interaction between the Madden–Julian Oscillation and the North Atlantic Oscillation. Nature 455 (7212), 523–527.

Collins, M., 2009. Evidence for changing flood risk in New England since the late 20th century. J. Am. Water Resour. Assoc. 45 (1), 1–12.

Daskalov, G., 2003. Long-term changes in fish abundance and environmental indices in the Black Sea. Mar. Ecol. – Progr. Ser. 255, 270.
Dickson, B., Osterhus, S., 2007. One hundred years in the Norwegian Sea. Norsk Geogr. Tidsskr. – Norw. J. Geogr. 61, 75.
Dima, Lohmann, 2010. Evidence for two distinct modes of large-scale ocean circulation changes over the last century. J. Climate. 23 (1), 5–16.
Flandrin, P., Rilling, G., Gonçalvès, P., 2004. Empirical mode decomposition as a filter bank. IEEE Signal Process. Lett. 11, 112–114.
Franceschini, S., Tsai, C.W., 2010. Application of Hilbert–Huang transform method for analyzing toxic concentrations in the Niagara River. J. Hydrol. Eng. 15 (2), 90–96.
Fritier, N., Massei, N., Laignel, B. Durand, A., Deloffre, J., Fournier, M., 2010. Links between NAO fluctuations and interannual variability of precipitation in the Seine river watershed. Global Change: Facing Risks and Threats to Water ressources. In: Proc. of the Sixth World FRIEND Conference, Fez, Morocco, October 2010, vol. 340. IAHS Publ. pp. 576–583.
Gledhill, R.J., 2003. Methods for investigating conformational change in biomolecular simulations, A dissertation for the degree of Doctor of Philosophy at the Department of Chemistry, the University of Southampton, p. 201.
Greene, C.H., Pershing, A.J., Conversi, A., Planque, B., Hannah, C., Sameoto, D., Head, E., Smith, P.C., Reid, P.C., Jossi, J., 2003. Trans-Atlantic responses of Calanus finmarchicus populations to basinscale forcing associated with the North Atlantic Oscillation. Prog. Oceanogr. 58 (2–4), 301–312.
Huang, N.E., Shen, Z., Long, S.R., Wu, M.L., Shih, H.H., Zheng, Q., Yen, N.C., Tung, C.C., Liu, H.H., 1998. The empirical mode decomposition and Hilbert spectrum for nonlinear and nonstationary time series analysis. Proc. R. Soc. Lond. 454, 903–995.
Huang, N.E., Wu, Z., 2008. A review on Hilbert–Huang transform: method and its applications to geophysical studies. Rev. Geophys. 46, RG2006. http://dx.doi.org/10.1029/2007RG000228.
Huang, Y., Schmitt, F., Lu, Z., Liu, Y., 2009. Analysis of daily river flow fluctuations using empirical mode decomposition and arbitrary order Hilbert spectral analysis. J. Hydrol. 373 (2009), 103–111.
Hurrell, J.W., Van Loon, H., 1997. Decadal variations in climate associated with the North Atlantic Oscillation. Clim. Change 36, 301–326.
Hurrell, J., Kushnir, Y., Ottersen, G., Visbeck, M., 2003. The North Atlantic Oscillation: climatic significance and environmental impact. Geophys. Monogr. (Am. Geophys. Union) 134, 1–35.
Keim, B.D., Muller, R.A., Stone, G.W., 2004. Spatial and temporal variability of coastal storms in the North Atlantic Basin. Mar. Geol. 210 (1–4), 7–15.
Kim, D., Oh, H.S., 2009. EMD: a package for empirical mode decomposition and Hilbert spectrum. R J. 1 (1), 40–46.
Kingston, D.G., McGregor, G.R., Hannah, D.M., Lawler, D.M., 2007. Large-scale climatic controls on new England River flow. J. Hydrometeor. 8, 367–379. http://dx.doi.org/10.1175/JHM584.1.
Labat, D., 2005. Recent advances in wavelet analyses: Part 1. A review of concepts. J. Hydrol. 314, 275–288.
Labat, D., Godderis, Y., Probst, J.L., Guyot, J.L., 2004. Evidence for global runoff increase related to climate warming. Adv. Water Resour. 2004, 631–642.
Lomas, M.W., Bates, N.R., 2004. Potential controls on interannual partitioning of organic carbon during the winter/spring phytoplankton bloom at the Bermuda Atlantic time-series study (BATS) site. Deep Sea Res., Part I 51 (11), 1619–1636.
Lee, T., Ouarda, T.B.M.J., 2011. Prediction of climate nonstationary oscillation processes with empirical mode decomposition. J. Geophys. Res. 116, D06107. http://dx.doi.org/10.1029/2010JD015142, 2011.
Lee, T., Ouarda, T.B.M.J., 2010. Long-term prediction of precipitation and hydrologic extremes with nonstationary oscillation processes. J. Geophys. Res. 115, D13107. http://dx.doi.org/10.1029/2009JD012801.
McCabe, G., Wolock, D., 2002. A step increase in streamflow in the conterminous United States. Geophys. Res. Lett. 29 (24), 2185.
Macdonald, R.W., Harner, T., Fyfe, J., 2005. Recent climate change in the Arctic and its impact on contaminant pathways and interpretation of temporal trend data. Sci. Total Environ. 342 (1–3), 5–86.
McMahon, T.A., Vogel, R.M., Peel, M.C., Pegram, G.G.S., 2007. Global streamflows – Part 1: characteristics of annual streamflows. J. Hydrol. 347 (3–4), 243–259.
Mares, I., Mares, C., Mihailescu, M., 2002. NAO impact on the summer moisture variability across Europe. Phys. Chem. Earth. 27 (23–24), 1013–1017.
Massei, N., Durand, A., Deloffre, J., Dupont, J., Valdes, D., Laignel, B., 2007. Investigating possible links between the North Atlantic Oscillation and rainfall variability in northwestern France over the past 35 years. J. Geophys. Res. – Atmos. 112, 1–10.
Massei, N., Laignel, B., Deloffre, J., Mesquita, J., Motelay, A., Lafite, R., Durand, A., 2010. Long-term hydrological changes of the Seine river flow (France) and their relation to the North-Atlantic Oscillation over the period 1950–2008. Int. J. Climatol. 30, 2146–2154. http://dx.doi.org/10.1002/joc.2022 (special issue).
Massei, N., Laignel, B., Rosero, E., Motelay-Massei, A., Deloffre, J., Yang, Z.-L., Rossi, A., 2011. A wavelet approach to the short-term to pluridecennal variability of streamflow in the Mississippi river basin from 1934 to 1998. Int. J. Climatol. 31, 31–43. http://dx.doi.org/10.1002/joc.1995.
Parsons, L.S., Lear, W.H., 2001. Climate variability and marine ecosystem impacts: a North Atlantic perspective. Prog. Oceanogr. 49 (1–4), 167–188.
Peel, M.C., McMahon, T.A., 2006. Recent frequency component changes in interannual climate variability. Geophys. Res. Lett. 33, L16810. http://dx.doi.org/10.1029/2006GL025670.
Rogers, J.C., 1997. North Atlantic storm track variability and its association to the North Atlantic Oscillation and climate variability of northern Europe. J. Climate 10, 1635–1647.
Serreze, M., Walsh, J., Chapin, F., Osterkamp, T., Dyurgerov, M., Romanovsky, V., Oechel, W., Morison, J., Zhang, T., Barry, R., 2000. Observational evidence of recent change in the northern high-latitude environment. Clim. Change 46, 207.
Slimani, S., Massei, N., Mesquita, J., Valdes, D., Fournier, M., Laignel, B., Dupont, J.P., 2009. Combined climatic and geological forcings on the spatio-temporal variability of piezometric levels in the chalk aquifer of Upper Normandy (France) at pluridecennal scale. Hydrogeol. J.. http://dx.doi.org/10.1007/s10040-009-0488-1.
Sole, J., Turiel, A., Estrada, M., Llebot, C., Blasco, D., Camp, J., Delgado, M., Fernandez-Tejedor, M., Diogene, J., 2009. Climatic forcing on hydrography of a Mediterranean bay (Alfacs Bay). Cont. Shelf. Res. 29 (15), 1786–1800.
Ulbrich, U., Christoph, M., Pinto, J., Corte-Real, J., 1999. Dependence of winter precipitation over Portugal on NAO and baroclinic wave activity. Int. J. Climatol. 19, 379–390.
Wu, Z., Huang, N.E., 2004. A study of the characteristics of white noise using the empirical mode decomposition method, Proc. Roy. Soc. London 1597-1611.
Wu, Z., Huang, N.E., 2009. Ensemble empirical mode decomposition: a noise-assisted data analysis method. AADA 1 (1), 1–41.